SUPPORTING INFORMATION

Dynamic states of the DNA repair enzyme AlkB regulate product release

Boris Bleijlevens, Tara Shivarattan, Emily Flashman, Yi Yang, Pete J. Simpson, Pertti Koivisto, Barbara Sedgwick, Christopher J. Schofield, Steve J. Matthews

Protein expression & purification

Recombinant *E. coli* AlkB was expressed as soluble protein in *E. coli* BL21 (DE3) bearing a recombinant plasmid derived from pET21b (Shivarattan et al., 2005). Over-expressed protein was full-length and C-terminally tagged with 6 histidines. Transformed cells were grown on plates containing 50 μg/ml carbenicillin. One litre of LB was inoculated with an overnight culture and incubated at 37 °C until cells reached an OD_{600} of 0.8. Protein expression was induced by addition of 0.4 mM IPTG (isopropylthiogalactopyranoside) and left at 37 °C for a further 4-6 hours. Cells were harvested and re-suspended in binding buffer (20 mM Tris-HCl (pH 8.0), 5 mM NaCl, 5 mM imidazole). Following lysis (by manual French press or sonication), the supernatant containing AlkB was loaded onto a Ni-NTA column (Qiagen) equilibrated with binding buffer. Two washes (25 mM and 50 mM of imidazole) were carried out prior to elution in 150 mM imidazole. The protein purity was checked by SDS-PAGE, protein yields were ~10 mg/L of bacterial culture. C-terminally tagged AlkB was active in demethylating DNA with an activity similar to N-terminally tagged protein. ^{15}N labelling was done in M9 minimal media containing 0.7 g/L $^{15}NH_4Cl$. The yield of ^{15}N-labelled AlkB was ~15 mg/L. Protein concentrations were measured using the Bradford method or measuring the absorption at 280 nm (ε_{280} = 31 mM^{-1} cm^{-1}).

The sequence encoding N-terminally truncated human $PHD2_{181-426}$ was sub-cloned into pET-24a, and recombinant protein was expressed in *E. coli* BL21(DE3) cells by induction with 0.5mM IPTG for 3-4 hours at 37°C. Cells were harvested and lysed by sonication in 100mM MES pH 5.8, and the supernatant loaded onto a cation exchange column. $PHD2_{181-426}$ was eluted with an increasing NaCl gradient, and further purified by size exclusion chromatography. Protein purity was typically >95%, as determined by SDS-PAGE (McNeill et al., 2005).

NMR spectroscopy

Sample preparation

AlkB samples were reconstituted with either Fe^{2+} or Co^{2+}, at equimolar protein to metal concentrations (based either on Bradford or A_{280}). Reconstitution with metal in the absence of organic cofactor (2OG or succinate) did not result in the formation of a stable complex and caused large precipitates. AlkB-metal complexes showed poorly dispersed NMR spectra (Fig S7A), indicative of incomplete folding and/or highly flexible domains. No, or very little, precipitation was observed if either 2OG or succinate were added to protein prior to the addition of metal (organic cofactor was added in 10-fold excess over protein). Also, metal would be added gradually to avoid precipitation. After formation, the Co complexes were more stable over time, most likely as the result of their inability to turnover O_2 and leading to self-inactivation. As expected, 2OG binding to AlkB is much tighter than succinate binding. When added at equal concentrations, only NMR spectra attributed to the 2OG complex were observed.

The NMR characteristics of cobalt reconstituted AlkB complexes were consistent with those observed for the analogous iron complexes. The 2D ^{1}H-^{15}N HSQC spectra are shown in Fig. S7. As in the Fe^{2+} spectra the 2OG complex shows a better dispersion of the resonances, indicating a better defined and more tightly folded complex. The presence of signals outside the classical diamagnetic window suggests that Co^{2+}, like Fe^{2+}, is bound in a paramagnetic state. Generally, Co^{2+} complexes ($3d^7$) can occur in low-spin ($S = 1/2$) or high-spin ($S = 3/2$) states. EPR analysis of the AlkB-Co^{2+}-2OG complex indicated binding of high-spin Co^{2+} to AlkB (not shown). The peaks outside the diamagnetic window in the 1D-^{1}H NMR spectra of both the Fe^{2+} and the Co^{2+} ternary complexes result from pseudo-contact shifts of protons in the vicinity of the high-spin metal centres. The ^{15}N-^{1}H HSQC NMR spectrum of the AlkB-Co^{2+}-2OG complex is better dispersed than that of the Fe^{2+} complex, showing ca. 200 peaks. In addition, the 2D ^{1}H-^{15}N HSQC spectrum of the binary AlkB-Co^{2+} complex is shown to illustrate the loss of tertiary structure compared to both the 2OG and the succinate binding complexes. Subsequent addition of succinate or 2OG to the binary complex resulted in increased spectral dispersion and folding of the protein complex.

Overview of broadened and shifted resonances in the AlkB-Fe^{2+}-succinate complex

Broadened resonances (13): Met49, Ala60, Thr71, Asn120, Arg121, Val146, Leu148, Phe154, Gly157, Leu184, Asn206, Gln211, Ala212.

Shifted resonances (25): Ala30, Arg47, Val59, Met61, Thr62, Cys64, Leu67, Gly68, Trp69, Thr70, Tyr109, Tyr122, Ala123, Gly125, Ala141, Gly149, His172, Gly180, Glu181, Phe185, Gly188, Gly195, Thr200, Tyr205, Gly213.

Estimation of the binding affinity of methylated DNA to the inhibited AlkB-Fe^{2+}-NOG complex

Since the inhibited AlkB-NOG complex is unable to catalyse demethylation of methylated DNA this complex was used to study DNA binding. Titration of meDNA (T-1meA-T) to the AlkB-Fe^{2+}-NOG complex induced various chemical shift changes that are in a slow-exchange regime on the NMR time-scale (Fig. S10). Slow ligand exchange is indicative of tight binding. Small chemical shift changes can be used to calculate an upper limit for the binding affinity. Such a calculation can only provide an upper limit for the binding affinity, the actual affinity in the complex may be well below this value.

For the estimation of the upper limit for the binding affinity we looked at peaks displaying small chemical shift changes (50 Hz in the proton domain, see fig S10). The k_d is defined as the ratio between the off-rate and the on-rate: $k_d = k_{off} / k_{on}$. Diffusion controlled interactions show an on-rate of 10^9 s^{-1} M^{-1}. To obtain a save estimate and to allow for non-productive collisions between DNA and protein we use a value for k_{on} of 10^8 $s^{-1}M^{-1}$. The observed minimal chemical shift change ($\Delta\nu$) of 50 Hz is used as the upper limit of the off-rate (k_{off}). Using these values we obtain an upper limit for the binding affinity of 500 nM. These data further confirm tight binding of methylated DNA to AlkB.

Equilibrium fluorescence spectroscopy

Methodology

Fluorescence spectra were recorded on a SPEX FluoroMax-3 fluorimeter (Jobin Yvon HORIBA) using a 4x4 mm quartz cuvette (sample volume ~ 300 µl) at 24°C. Tryptophans in AlkB were excited at 290 nm and emission spectra were recorded from 300 – 400 nm at 1 nm resolution (data collection 1 s/data point). Slit widths at excitation and emission wavelengths were 5 nm. A stock of 50 µM AlkB in 20 mM Tris-HCl, pH 7.6 was diluted in distilled H_2O to a concentration of 1 µM. Tryptophan fluorescence was quenched with acrylamide to assess exposures of tryptophans to solvent (Eftink and Ghiron, 1975; Eftink and Ghiron, 1981); intensities were corrected for dilution and radiation absorption by added quencher (Parker, 1968) using a molar extinction coefficient (ε_{290}) for acrylamide of 0.23 $M^{-1}cm^{-1}$ (Eftink and Ghiron, 1981). Dynamic, diffusion controlled quenching is characterized by the Stern-Volmer equation: $F_0/F = K_{SV}*[Q] + 1$, with F_0 the fluorescence emission in the absence of quencher, F the observed emission in the presence of quencher, [Q] the quencher concentration and K_{SV} the Stern-Volmer constant. A linear Stern-Volmer plot is indicative of the presence of one single class of fluorophore. In the case of multiple, non-equivalent fluorophores data can be plotted in a modified Stern-Volmer plot according to $F_0/(F_0-F) = 1/(f_a*K_{SV}*[Q]) + 1/f_a$ where the constant f_a indicates the fraction of accessible fluorophores.

Results

Tryptophan fluorescence was measured for the complexes of AlkB with metal, 2OG and succinate. To avoid issues of self-inactivation and sample heterogeneity of the AlkB-Fe^{2+} complex, the stable AlkB-Co^{2+} complex was used in these experiments. Fluorescence spectra of AlkB complexes displayed an emission band with a maximum at 338 nm, typical for Trp residues embedded in a protein matrix. AlkB contains four Trp residues (Trp11, Trp69, Trp89, and Trp178) that most likely all contribute to the observed fluorescence spectrum. The emission intensity of the AlkB-Co^{2+}-succinate complex was nearly 25% higher than that of the AlkB-Co^{2+}-2OG complex, indicating structural dissimilarities (Fig. S8A). As a result of the more dynamic nature of the succinate complex, the tryptophan fluorescence is probably less efficiently quenched by the surrounding protein matrix, resulting in an increased fluorescence for this state.

Changes in the microenvironment of tryptophan residues and their solvent accessibility were addressed by equilibrium fluorescence quenching experiments using acrylamide as a quencher (Eftink and Ghiron, 1975). As shown in the Stern-Volmer plot in Fig. S8B, the fluorescence intensity of the AlkB-Co^{2+}-succinate complex correlates linearly with quencher concentration. The AlkB-Co^{2+}-2OG complex however, showed a clear deviation from linearity towards the [Q]-axis. Such a deviation indicates the presence of multiple fluorophores with different quencher efficiencies. Since AlkB contains four Trp residues the occurrence of more than one class of fluorophores is not surprising. The presence of multiple fluorophores can be accounted for by plotting the data in a modified Stern-Volmer plot, which indeed allowed linear fitting of all data (Fig. S8C). The fit for the AlkB-Co^{2+}-succinate complex crosses the y-axis at a value of 1 (= $1/f_a$), indicating that for this complex the fraction of fluorophores accessible to quencher is 1. This means that, at infinite quencher concentration, all fluorophores are equally accessible. Conversely, for the AlkB-Co^{2+}-2OG complex the y-value at infinite quencher concentration is 1.37, or an accessibility fraction of 0.73. This observation can be explained by the following two extremes: either one tryptophan is completely shielded from quencher by the protein matrix while the other three are still completely accessible, or all four tryptophans are equally shielded from quencher. Even though quenching patterns for multi-tryptophan proteins are difficult to analyze in detail without more precise knowledge of fluorescence lifetimes and relative fluorophore contributions, qualitative information can still be extracted. Acrylamide is uncharged and fairly small and penetrates deeply into a protein to collisionally quench even the most shielded tryptophans (Eftink and Ghiron, 1975). Therefore, reduced fluorophore accessibility is best understood as a decrease in dynamics of the protein matrix. Consequently, these fluorescence quenching results show that in solution AlkB adopts two main structural conformations, an open and dynamic state (for the succinate complex) and a more tightly folded state (in case of the 2OG complex).

Isothermal titration calorimetry (ITC)

apoAlkB (20 µM, ~ 2.4 mL) was mixed with co-factor (2OG or succinate, 1 mM), ascorbate (2 mM) and DTT (2 mM). The mixture was thoroughly degassed (10 min) and a freshly prepared stock solution (10 mM) of $FeSO_4$, dissolved in 100 mM ascorbate, was added in slight excess (end concentration 30 µM). The reconstituted complex was degassed for a further 5 min and transferred into the ITC measurement cell. The cell was immediately closed with the syringe containing the ligand solution. The system was allowed to equilibrate for 30 to 60 min before starting the measurement. The reaction of DTT and ascorbate with residual oxygen in the sample generated significant amounts of heat causing baseline drifting. This reaction was used to our advantage as in a closed system residual oxygen was removed resulting in anaerobic conditions. After 30 to 60 min all remaining O_2 would have reacted and the baseline stabilised. The titration was only started after a stable baseline had been obtained. Ligand (200 µM) was added (5 or 10 µl per addition). Ligand solution also contained ascorbate (2 mM), DTT (2 mM), co-factor (1 mM) to mimick the protein sample as closely as possible and avoid mixing effects. The ligand solution was degassed prior to filling the syringe. Since the syringe was loaded before filling of the ITC cell (to allow quick closure of the cell) the oxygen scavenging reaction had even more time to complete, ensuring anaerobicity of the ligand solution.

	k_b (nM)	**ΔH (kcal/mol)**	**T * ΔS (kcal/mol)**	**ΔG (kcal/mol)**
AlkB-2OG + TmeAT (high affinity)	9.8 ± 5.1	-55 ±16	-43 ± 16	-12
AlkB-2OG + TmeAT (low affinity)	287 ± 16	-9 ± 1.3	-0.1 ± 1.3	-8.9
AlkB-succ. + TmeAT (high affinity)	16.9 ± 11.7	-35 ± 2	-24.2 ± 2.7	-11
AlkB-succ. + TmeAT (low affinity)	454 ± 260	-10.5 ± 1.5	-1.7 ± 2	-8.8
AlkB-succ. + TTCTT	885 ± 115	-26 ± 11	-18 ± 11	-8

Table 1. Thermodynamic constants as obtained from fitting of the binding isotherms measured in the ITC experiments recorded at 298 K (presented in Figure 4). Binding of methylated ssDNA (T-1meA-T) to AlkB complexes was fitted as two independent binding events, one with high affinity and one with lower affinity. Binding of unmethylated ssDNA (TTCTT) was fitted as one binding event.

REFERENCES SUPPORTING INFORMATION

Compton, L.A. and Johnson, W.C., Jr. (1986) Analysis of protein circular dichroism spectra for secondary structure using a simple matrix multiplication. *Anal Biochem*, **155**, 155-167.

Eftink, M.R. and Ghiron, C.A. (1975) Dynamics of a protein matrix revealed by fluorescence quenching. *Proc Natl Acad Sci U S A*, **72**, 3290-3294.

Eftink, M.R. and Ghiron, C.A. (1981) Fluorescence quenching studies with proteins. *Anal Biochem*, **114**, 199-227.

McNeill, L.A., Flashman, E., Buck, M.R., Hewitson, K.S., Clifton, I.J., Jeschke, G., Claridge, T.D., Ehrismann, D., Oldham, N.J. and Schofield, C.J. (2005) Hypoxia-inducible factor prolyl hydroxylase 2 has a high affinity for ferrous iron and 2-oxoglutarate. *Mol Biosyst*, **1**, 321-324.

Parker, C.A. (1968) *Photoluminescence of Solutions*. Elsevier, New York, N.Y.

Shivarattan, T., Chen, H.A., Simpson, P., Sedgwick, B. and Matthews, S. (2005) Resonance assignments of Escherichia coli AlkB: a key 2-oxoglutarate and Fe(II) dependent dioxygenase of the adaptive DNA-repair response. *J Biomol NMR*, **33**, 138.

Whitmore, L. and Wallace, B.A. (2004) DICHROWEB, an online server for protein secondary structure analyses from circular dichroism spectroscopic data. *Nucleic Acids Res*, **32**, W668-673.

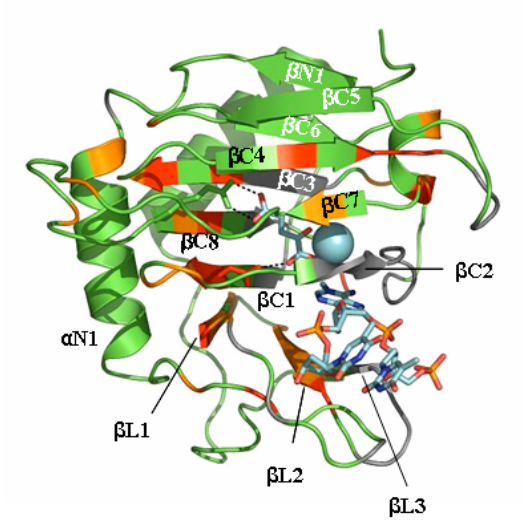

A) Dynamic residues in the succinate complex are coloured red (for severely broadened resonances) and orange (for resonances displaying chemical shift changes)

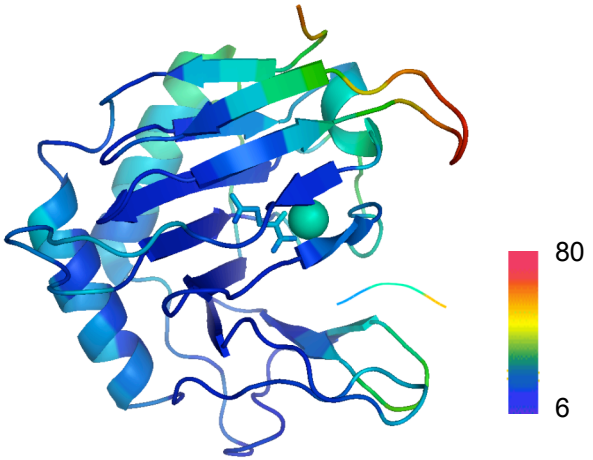

B) 2FD8: AlkB-Fe^{2+}-2OG + TmeAT

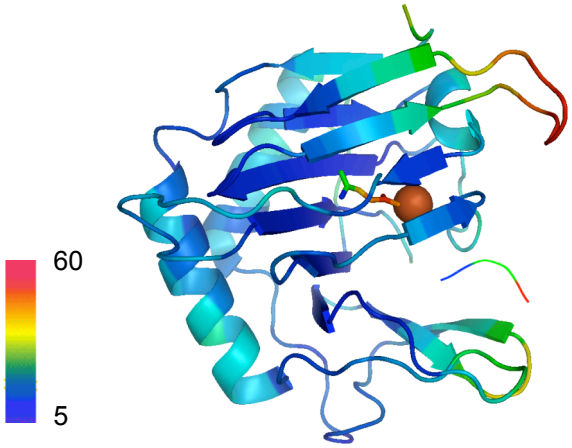

C) 2FDG: AlkB-Fe^{2+}-succ + TmeAT

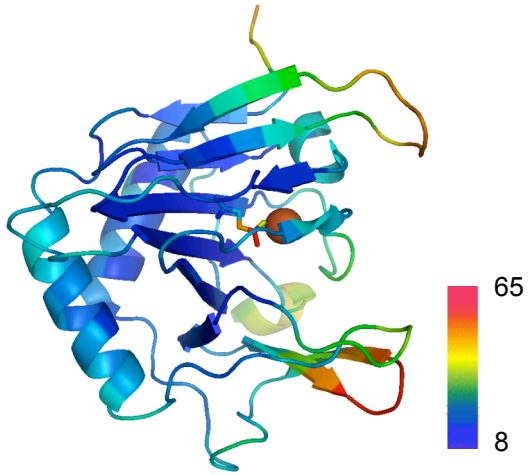

D) 2FDJ: AlkB-Fe^{2+}-succ

FIGURE S6. Comparison of increasingly dynamic residues in the AlkB complexes. (A) Dynamic changes in the AlkB-succinate complex as measured in solution by NMR spectroscopy. (B-D) B-factors in the X-ray structures of (B) the 2OG complex and the succinate complexes (C) with and (D) without meDNA. The Fe ions (spheres) and cofactors (stick) are coloured according to B-factor. Water molecules are not shown. Cold, more rigid regions of the protein are coloured blue whereas hotter, flexible parts of the protein (with higher B-factors) are red.

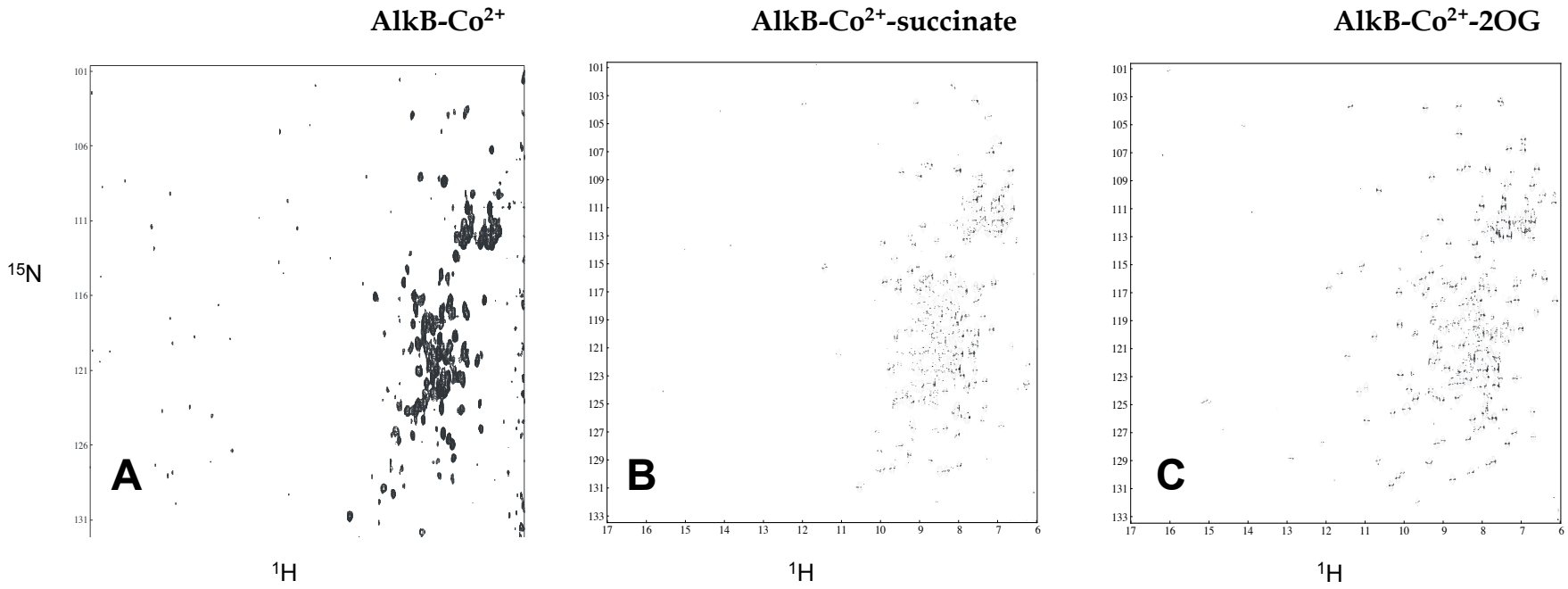

FIGURE S7. ^{15}N-^{1}H HSQC NMR spectra of the various Cobalt complexes. (A) AlkB-Co^{2+}, (B) AlkB-Co^{2+}-succinate, and (C)AlkB -Co^{2+}-2OG.

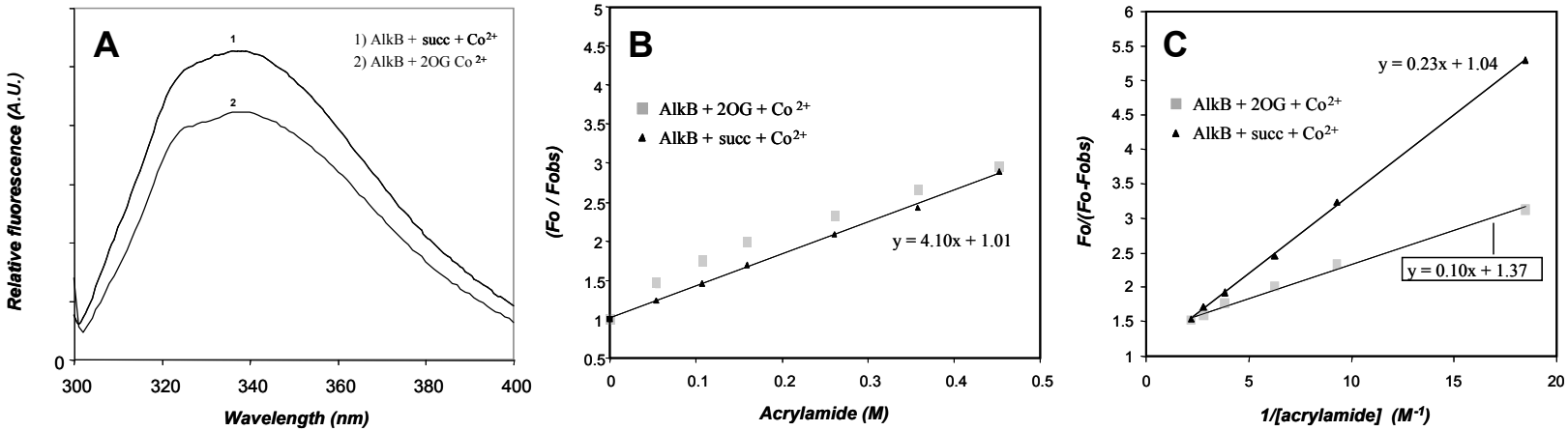

FIGURE S8. The effect of b inding of co -substrate (2OG), and co -product (succinate) to AlkB on the steady -state tryptophan fluorescence. (A) Relative fluorescence intensities of the two complexes. The fluorescence of the various complexes was quenched with increasing concentrations of acrylamide and the relative intensities are p lotted in (B) a Stern -Volmer plot and (C) a modified Stern -Volmer plot .

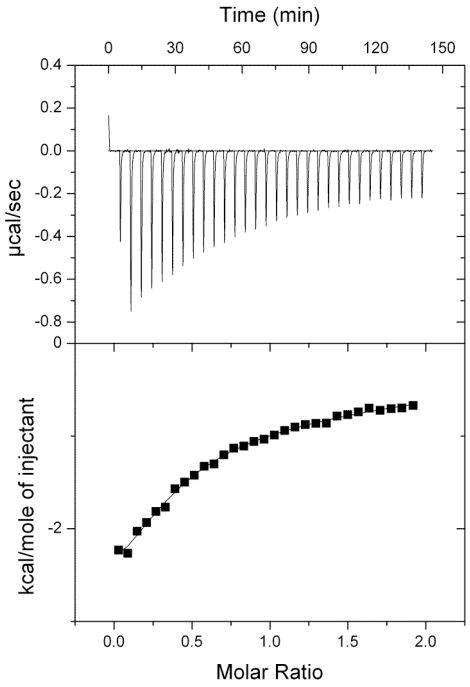

FIGURE S9. Isothermal calorimetric titration of apo AlkB with demet hylated DNA (TTCTT). A concentrated solution of DNA (1 mM) is titrated to apo AlkB (100 _M). Data were fitted according to a model assuming two independent binding sites with K_{b1} = 15 µM and K_{b2} = 500 µM.

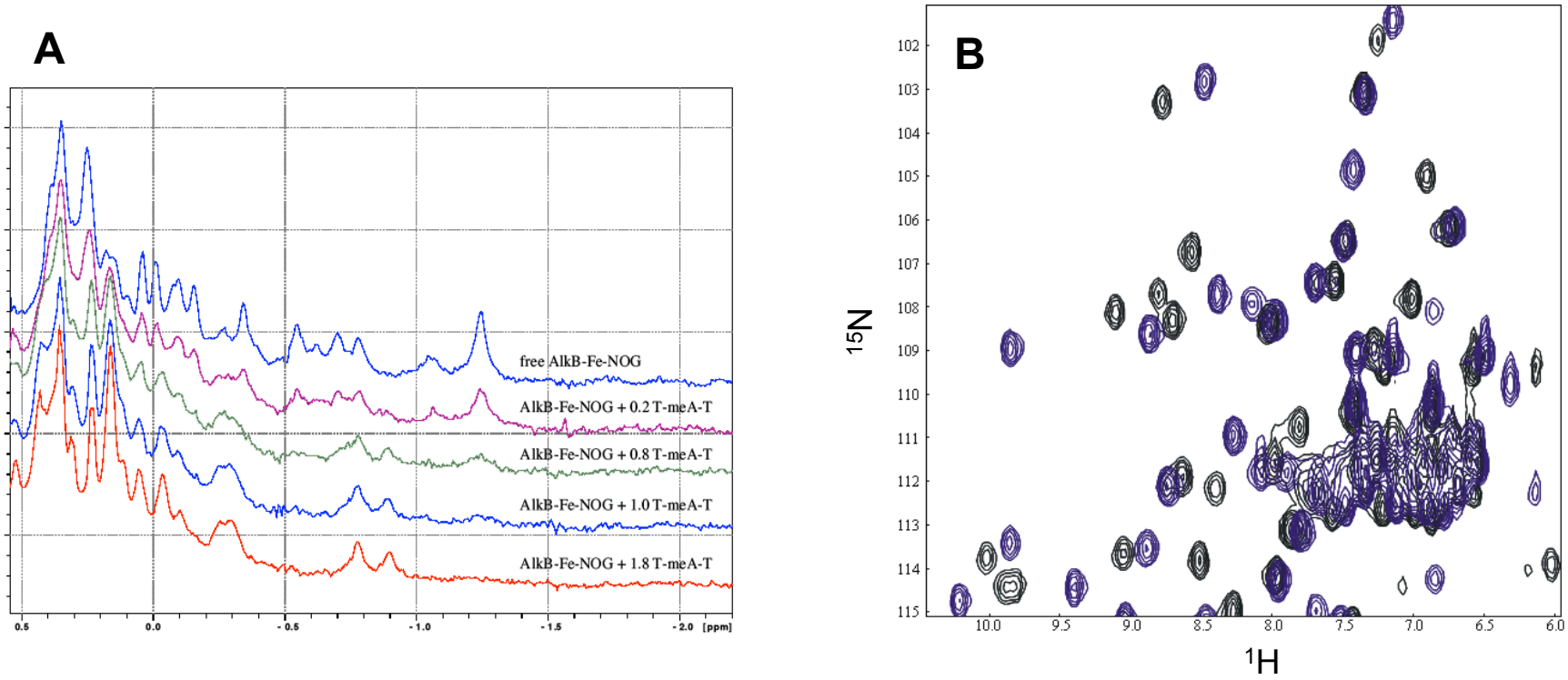

FIGURE S10. (A) Methyl region of 1D ^{1}H-NMR spectra of the AlkB -Fe complex inhibited with N -oxalylglycine (NOG) and incubated with increasing amounts of methylated DNA (TmeAT). (B) Overlay of (part of) the 2D ^{1}H-^{15}N HSQC spectra of free AlkB -Fe -NOG (blue) a nd AlkB -Fe- NOG incubated with TmeAT (black, ratio 1: 1.8). Spectra are recorded at 500 MHz at 303 K. The AlkB -TmeAT complex occurs in the slow exchange regime on the NMR timescale, indicating tight binding.

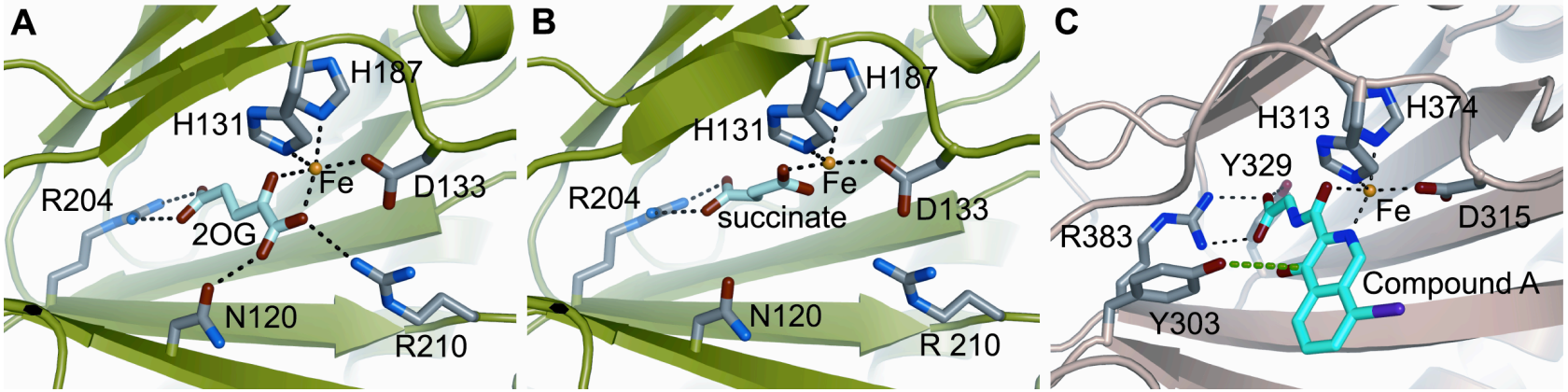

FIGURE S11 . X-ray structures of the active sites of AlkB with (A) co -substrate 2OG and (B) co - product succinate bound in the active site, demonstrating the loss of contact between Asn120 and the organic cofactor. (C) The active site of PHD2 binding the inh ibitor Compound A (McDonough et al, PNAS 2006), illustrating that Tyr303 is located such that it can perform a similar role as Asn120 in AlkB. Figure prepared from PDB files 2FD8 / 2FDG (for AlkB) and 2G1M (for PHD2).

Spectral overlays of ^{15}N-^{1}H HSQC NMR spectra of complexes of AlkB-Co^{2+} complexes

In red: AlkB-Co^{2+}-succinate

In black: AlkB-Co^{2+}-2OG

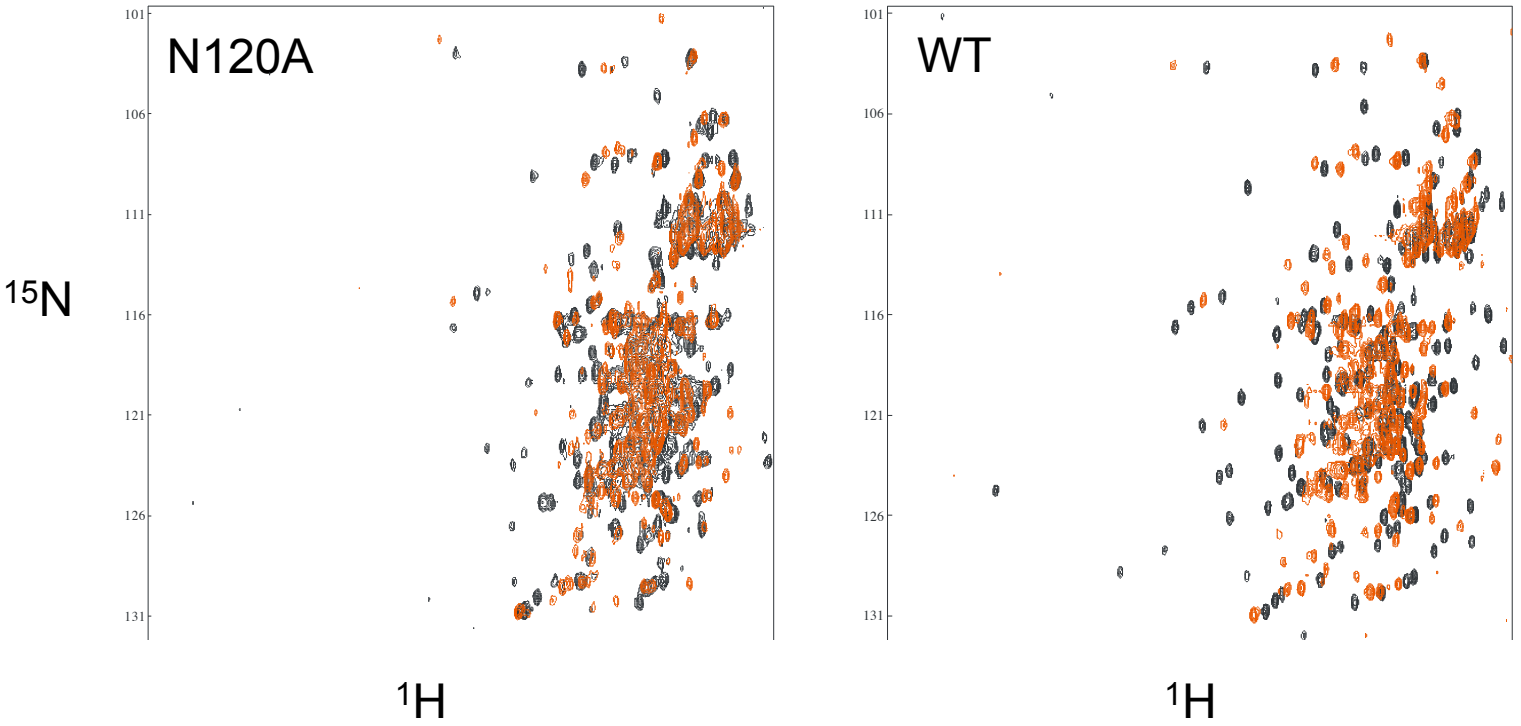

FIGURE S12 . ^{15}N-^{1}H HSQC NMR spectra of the AlkB -Co^{2+}-2OG the AlkB -Co^{2+}-succinate complexes of WT AlkB and the N120A mutant. Although the A120AlkB -2OG complex shows a slightly better dispersed spectrum than the A120AlkB -succinate complex the effect is not quite as pronounced as in WT Alk B. 2OG makes more contacts with the protein than with residue 120, for example with the metal site and also with Arginine 210 (see also Fig. S1 1), explaining the sli ght increase in folding of the N 120A-2OG complex com pared to the N 120A-succinate complex. Nonetheless, the spectrum is clearly less dispersed than that of the WT -2OG complex .